

Similarity of thermodynamic properties of Heisenberg model on triangular and kagome lattices

P. Prelovšek^{1,2} and J. Kokalj^{3,1}

¹*Jožef Stefan Institute, SI-1000 Ljubljana, Slovenia*

²*Faculty of Mathematics and Physics, University of Ljubljana, SI-1000 Ljubljana, Slovenia*

³*Faculty of Civil and Geodetic Engineering, University of Ljubljana, SI-1000 Ljubljana, Slovenia*

Derivation of a reduced effective model allows for a unified treatment and discussion of the J_1 - J_2 Heisenberg model on a triangular and kagome lattice. Calculating thermodynamic quantities, i.e. the entropy $s(T)$ and uniform susceptibility $\chi_0(T)$, numerically on systems up to effectively $N = 48$ sites we show by comparing to full-model results that low- T properties are well represented within the reduced model. Moreover, we find in the spin-liquid regime similar variation of $s(T)$ as well as $\chi_0(T)$ in both models down to $T \ll J_1$. In particular, the spin liquid appears to be characterized by Wilson ratio vanishing at low T , indicating on the low-lying singlet dominating over the triplet excitations.

Introduction. Studies of possible quantum spin-liquid (SL) state in spin models on frustrated lattices have a long history, starting with the Anderson's conjecture [1] for the Heisenberg model on a triangular lattice. In last two decades theoretical efforts have been boosted by the discovery of several classes of insulators with local magnetic moments [2–4], which do not reveal long-range order (LRO) down to lowest temperatures T . The first class are compounds, as the herbertsmithite $\text{ZnCu}_3(\text{OH})_6\text{Cl}_2$ [5], which can be represented with Heisenberg $S = 1/2$ model on kagome lattice, being the subject of numerous experimental studies [6–9], now including also related materials [10–15] confirming the SL properties, at least in a wide $T > 0$ range. Another class are organic compounds, as κ -(ET) $_2\text{Cu}_2(\text{CN})_3$ [16–19], where the spins reside on a triangular lattice. Recently, the charge-density-wave system 1T-TaS $_2$, which is a Mott insulator without magnetic LRO and shows spin fluctuations at $T > 0$ [20–23], has been added into this family.

Numerical [24–26] and analytical [27] studies of the nearest-neighbor (nn) quantum Heisenberg model (HM) on a triangular lattice (TL) confirm a spiral long-range order (LRO) with spins pointing in 120° tilted directions. Introducing the next-nearest-neighbor (nnn) coupling $J_2 > 0$ enables the SL ground state (g.s.) in the part of the phase diagram [28–34]. There is even more extensive literature on the HM on the kagome lattice (KL) confirming the absence of g.s. LRO order [35–39]. The prevailing conclusion of numerical studies of the g.s. and lowest excited states is that HM on KL has a finite spin triplet gap Δ_t [39–42] (with some evidence pointing also to gapless SL [38, 43]), but much smaller or vanishing singlet gap $\Delta_s \ll \Delta_t$ [35, 42, 44–48]. On the other hand, extensions into the J_1 - J_2 model [43, 49] with $J_2 > 0$ again leads towards g.s. with magnetic LRO. Still, HM on both lattices in their respective SL parameter regimes have been studied and considered separately, not recognizing or stressing their similarity.

In this Letter, with the goal to put extended J_1 - J_2 HM on TL and KL on a common ground, we construct a re-

duced effective model (EM), which is based on keeping only the lowest doublet $S = 1/2$ states in a single triangle. Such an EM has been previously introduced for KL [35, 36, 50] but not yet studied in connection with the TL and also not employed to evaluate $T > 0$ properties. While such an EM has an evident advantage of reduced number of states in an exact-diagonalization (ED) study and hence allowing for somewhat larger lattices (in our study up to $N = 48$ sites), it allows also an insight into the character of low-energy excitations, being now separated into spin (triplet) and chirality (singlet) ones. The main focus of this work is on the numerical evaluation of thermodynamic quantities, i.e. entropy density $s(T)$ and uniform susceptibility $\chi(T)$, within the SL parameter regimes, approached before mostly by high- T expansion [44–47, 51–53] and only recently with numerical methods adequate for lower $T \ll J_1$, both on TL [54] and KL [48].

Wilson ratio. Our results in the following reveal that in both lattices (in the SL regime) $s(T)$ and $\chi_0(T)$ are very similar in a broad range of T . Here very convenient quantity is T -dependent modified Wilson ratio $R(T)$, defined as

$$R = 4\pi^2 T \chi_0 / (3s), \quad (1)$$

and is equivalent (assuming theoretical units $k_B = g\mu_B = 1$) to the standard ($T = 0$ constant) Wilson ratio in the case of Fermi-liquid behavior $s = C_V = \gamma T$. Definition Eq. (1) is convenient since it has meaningful T dependence due to monotonously increasing $s(T)$, having also finite high- T limit $R_\infty = \pi^2 / (3 \ln 2) = 4.75$. Moreover, it can differentiate between quite distinct $T \rightarrow 0$ scenarios: a) in the case of LRO at $T \rightarrow 0$ one expects in 2D (isotropic HM) $\chi_0(T \rightarrow 0) \sim \chi_0^0 > 0$ but $s \propto T^2$ [55], so that $R_0 = R(T \rightarrow 0) \rightarrow \infty$, b) in a gapless SL with large spinon Fermi surface one would expect Fermi-liquid-like $R_0 \sim 1$ [3, 19, 22], c) $R_0 \ll 1$ or a decreasing $R(T \rightarrow 0) \rightarrow 0$ would indicate a dominating low-energy singlet excitation over the triplet ones [3, 42]. In the following we find in the SL regime numerical evidence for

the last scenario, which within the EM we attribute to low-lying chiral fluctuations being a hallmark of SL.

Effective model. We consider the isotropic $S = 1/2$ extended J_1 - J_2 Heisenberg model,

$$H = J_1 \sum_{\langle kl \rangle} \mathbf{S}_k \cdot \mathbf{S}_l + J_2 \sum_{\langle\langle kl \rangle\rangle} \mathbf{S}_k \cdot \mathbf{S}_l, \quad (2)$$

on the TL and KL, where $J_1 > 0$ and J_2 refer to nn and nnn exchange couplings, respectively. The role of $J_2 > 0$ in TL is to destroy the 120° LRO allowing for a SL [28–30, 32, 54], while for KL it has the opposite effect [49]. Further we set $J_1 = J = 1$ as an energy scale. Model (2) on both lattices can be represented as coupled basis triangles [35, 36, 50] where we keep in the construction of the EM four degenerate $S = 1/2$ states (local energy $E_0 = -3/4$), neglecting higher $S = 3/2$ states (local $E_1 = 3/4$),

$$\begin{aligned} |\uparrow \pm\rangle &= \frac{1}{\sqrt{3}} [|\downarrow\uparrow\uparrow\rangle + e^{\pm i\phi} |\uparrow\downarrow\uparrow\rangle + e^{\mp i\phi} |\uparrow\uparrow\downarrow\rangle], \\ |\downarrow \pm\rangle &= \frac{1}{\sqrt{3}} [|\uparrow\downarrow\downarrow\rangle + e^{\mp i\phi} |\downarrow\downarrow\downarrow\rangle + e^{\mp i\phi} |\downarrow\uparrow\downarrow\rangle], \end{aligned} \quad (3)$$

where $\phi = 2\pi/3$, \uparrow, \downarrow are (new) spin states and \pm refer to local chirality. One can rewrite Eq.(2) into the new basis acting between nn triangles $\langle i, j \rangle$, using new local $S = 1/2$ spin operators \mathbf{s}_i (i referring to triangles) and pseudospin (chirality) operators τ_i . The EM can be then written as,

$$H = \frac{1}{2} \sum_{i,d} \mathbf{s}_i \cdot \mathbf{s}_j (D + \mathcal{H}_{ij}^d), \quad (4)$$

$$\mathcal{H}_{ij}^d = F_d \tau_i^+ \tau_j^- + P_d \tau_i^+ + Q_d \tau_j^+ + T_d \tau_i^+ \tau_j^+ + \text{H.c.},$$

where directions $d = 1-6$ and $j = i + d$ run over nn sites of site i , and new lattice is again TL. We note that Eq. (4) corresponds to the one considered for simplest KL [35, 36], but it is valid also for TL and nnn J_2 . It is remarkable that the spin part remains $SU(2)$ invariant whereas the chirality part is not, i.e., it is of the XY form. Here we display only D and F_d terms,

$$\begin{aligned} D &= \frac{2}{9}J + \frac{1}{3}J_2, & F &= -\frac{4}{9}J + \frac{4}{3}J_2, & \text{TL} \\ D &= \frac{1}{9}J + \frac{2}{9}J_2, & F_d &= \frac{4}{9}e^{i\phi_d}J + \frac{8}{9}e^{-i\phi_d}J_2, & \text{KL} \end{aligned} \quad (5)$$

where $\phi_d = \pm 2\pi/3$ is alternating among bonds $d = 1-6$. Other terms with P_d, R_d, T_d are as well nonzero and are explicitly given in the Supplement [56]. In contrast to D, F_d , Eq. (6), their coupling averaged over nn bonds vanishes, e.g., $\bar{P} = (1/6) \sum_d P_d = 0$. This would indicate that such terms are less crucial, which is only partly true, as we test furtheron comparing results of the EM with the simplified EM (SEM), containing only D, F_d terms.

Eqs. (4),(6) yield some basic insight into the similarities and differences of HM on KL and TL. While $\chi_0(T)$

is governed entirely by \mathbf{s} operators, low- T entropy $s(T)$ (and specific heat) involves also chirality τ fluctuations. In TL at $J_2 = 0$ τ coupling is ferromagnetic and favors spiral 120° LRO. τ fluctuations are enhanced via $J_2 > 0$ reducing F and finally $F \rightarrow 0$ on approaching $J_2 \sim 0.3$. Still, before that P_d, Q_d, T_d terms become relevant and stabilize SL at $J_2 \sim 0.1$ [28–32]. It should be stressed that in TL a standard LRO requires ordering of \mathbf{s} and τ operators. On the other hand, KL at $J_2 = 0$ has complex and alternating F_d where $|\text{Im}F_d| < |\text{Re}F_d|$, indicating the absence of LRO. Here, $J_2 > 0$ reduces $|\text{Im}F_d|$ and on approaching $J_2 \sim 0.5$ one reaches real $F_d < 0$ connecting KL model to TL at $J_2 = 0$ and related LRO, as observed in numerical studies [49].

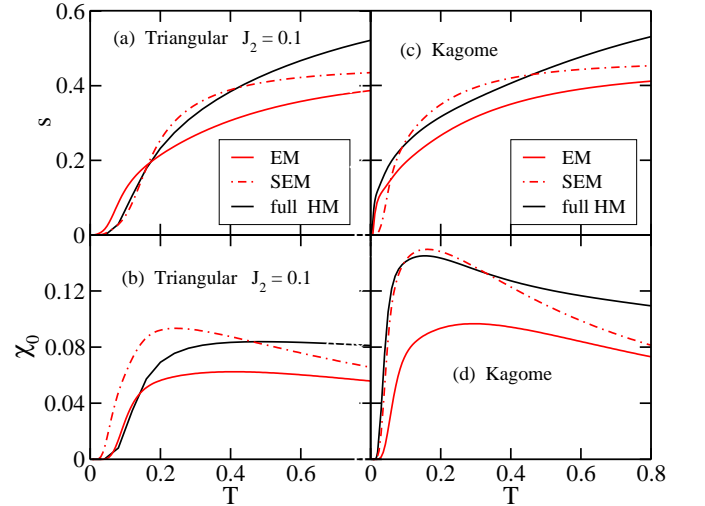


Figure 1. Results for the effective model (EM) and simplified effective model (SEM) for the triangular lattice, compared with the full HM. All results for are for $N = 30$ sites [54]: a) for entropy density $s(T)$ and b) uniform susceptibility $\chi_0(T)$. c) and d) same quantities for the kagome lattice, compared to full HM, all on $N = 42$ sites [48].

In the following we focus on the numerical evaluation of the thermodynamic $T > 0$ properties of EM and SEM. We calculate quantities entering the Wilson ratio, Eq. (1), i.e. the entropy density $s(T)$ and the uniform susceptibility $\chi_0(T)$. Both quantities are calculated (see definitions and details in [56]) via the finite-temperature Lanczos method (FTLM) [57–60], which has been recently used to calculate $T > 0$ static and dynamical properties of J_1 - J_2 HM of TL up to $N = 30$ sites [54], as well as thermodynamic $T > 0$ quantities on KL with up to $N = 42$ sites [48]. It should be reminded that for thermodynamic quantities involving only conserved quantities [59, 60] computer requirements are essentially equal as for ED g.s. determination and we are limited by the number of basis states. Since SEM has besides total s_{tot}^z conserved also τ_{tot}^z we can reach in this case $N = 48$ sites ($\tilde{N} = 16$ in reduced lattice), while for EM we use

up to $N = 42$ sites. Moreover, FTLM results are expected to become macroscopic (i.e. size independent) for higher $T > T_{fs}$. Here, the frustration works in favor of the method and we can reach $T_{fs} \ll 1$. Since the condition for T_{fs} is closely related to entropy and at given N , we can locate $s(T_{fs}) \lesssim 0.07$ for a given model (for gapped systems FTLM can be followed even to $T \rightarrow 0$).

Entropy and uniform susceptibility. Let us first benchmark results within the EM and SEM with the existing results for the full HM on TL and KL. In Figs. 1a,b we present $s(T)$ and $\chi_0(T)$, respectively, as obtained on TL for $J_2 = 0.1$ on $N = 30$ via FTLM on EM and SEM, compared with the full HM on the same size [54]. The qualitative behavior of both quantities within EM and SEM is quite similar at low $T < 0.4$, although EM (SEM) miss (as expected) $s(T)$ with increasing T , but apparently also some part of spin fluctuations reducing the value of $\chi_0(T)$. Still, the peak in $\chi_0(T)$ (and related spin gap $\Delta_s > 0$ at low T) are reproduced well within EM, and less satisfactory within SEM. Similar conclusions emerge from Figs. 1c,d where corresponding results are compared for the KL, where full-HM results for $s(T)$ and $\chi_0(T)$ are taken from study on $N = 42$ sites [48]. Here, EM clearly reproduces reasonably not only spin gap $\Delta_s \sim 0.1$ but also singlet excitations dominating $s(T \rightarrow 0)$, while apparently EM underestimates the value of $\chi_0(T)$.

After testing (S)EM with the full model, we present in Figs. 2,3 (S)EM results for $s(T)$ and $\chi_0(T)$ for both lattices as they vary with $J_2 > 0$. In Fig. 2a,b we follow the behavior on TL for different $J_2 = 0, 0.1, 0.15$. From the inflection point at $s(T \sim T_s)$ one can speculate on the coherence scale (in the case of LRO) or possible (singlet) excitation gap $\Delta_s \lesssim T_s$ (in the case of SL), at least provided that $T_s > T_{fs}$. On the other hand, an inflection point of $\chi_0(T \sim T_t)$ would indicate on the onset of spin coherence or spin (triplet) gap $T_t \lesssim \Delta_t$. Although the influence of $J_2 > 0$ does not appear large, it still introduces a qualitative difference. From this perspective $s(T)$ within EM at $J_2 = 0$ reveals higher $T_s \sim 0.12$ (even $T_s \sim 0.25$ for SEM) not excluding $s(T < T_s) \propto T^2$, consistent with a spiral LRO at $T = 0$. Still $T_s \sim T_{fs}$ within EM, so we can hardly make stronger conclusions in this case. On the other hand, for $J_2 = 0.1, 0.15$ where the SL can be expected [28, 32, 33] the EM reveals smaller $T_s \sim 0.05$ which is the signature of the singlet gap (which could still be finite-size dependent). More important, results confirm large residual entropy $s \sim 0.1 = 0.14s_{max}$ even at $T \sim 0.1$. This is in contrast with $\chi_0(T)$ in Fig. 2b which reveal T -variation weakly dependent on J_2 . While for $J_2 = 0$ the drop at $\chi_0(T < T_t)$ is the signature of finite-size spin gap (where due to LRO $\chi_0^0 = \chi_0(T \rightarrow 0) > 0$ is expected) $J_2 = 0.1, 0.15$ cases are different since vanishing χ_0^0 could confirm the spin triplet gap $\Delta_t > 0.1$ beyond the finite-size effects, i.e. $T_t \sim 0.1 > T_{fs}$. The result of SEM are to some extent similar to EM, but they over-amplify the tendency to LRO for all J_2 .

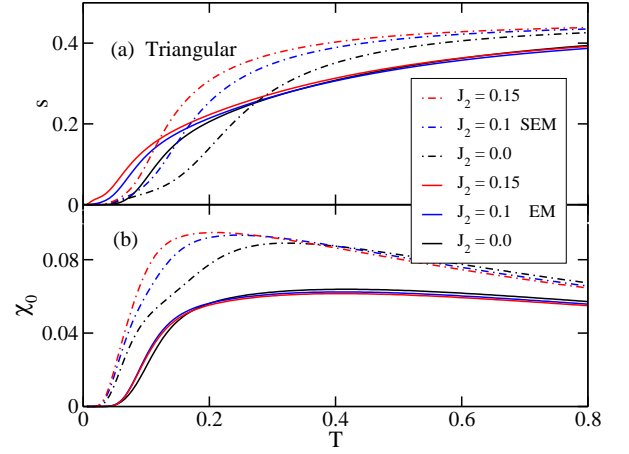


Figure 2. Results within EM and SEM on triangular lattice for different $J_2 = 0, 0.1, 0.15$; a) for $s(T)$, and b) $\chi_0(T)$.

In Figs. 3a,b we present the same quantities for the case of KL, now for $J_2 = 0, 0.2, 0.4$. The effect of $J_2 > 0$ is opposite, since it is expected to recover the LRO at $J_2 \sim 0.4$ [49], with 120° spin orientation analogous to $J_2 = 0$ TL. The largest low- T entropy $s(T)$ is found for KL with $J_2 = 0$. Moreover, EM here yields a quantitative agreement with the full HM [48], revealing large remanent $s(T)$ due to singlet (chirality) excitations down to $T \sim 0.01$ [42]. Here, in comparison to EM the SEM fails to distribute the drop of $s(T)$ over a wider T range, but nevertheless reveals large $s(T)$ down to $T \sim 0.05$. The evident effect of $J_2 > 0$ is to reduce $s(T)$ and finally leading $s(T) \propto T^2$ at large $J_2 \sim 0.4$ which should be a regime of magnetic LRO [49]. Again, at $J_2 = 0$ in contrast to entropy $\chi_0(T)$ has well pronounced downturn (both EM and SEM) at $T \sim 0.1$ consistent with the triplet gap $\Delta_t \sim 0.1$ found in most other numerical studies [42, 45–48]. Introducing $J_2 > 0$ does not change $\chi_0(T)$ qualitatively, although SEM indicates on saturation of χ_0^0 (consistent with LRO at $T = 0$).

Wilson ratio - results. To calculate $R(T)$, Eq. (1), let us first use available results for full HM for TL [54] and KL [48], comparing in Fig. 4 also the result for unfrustrated HM on a square lattice [54]. Here, we take into account data for $T > T_{fs}$, acknowledging that T_{fs} are quite different (taking $s(T_{fs}) \sim 0.1$ as criterion) for these systems, representative also for the degree of frustration. Fig. 4 already confirms different scenarios for $R(T)$. On a square-lattice HM starting from high- T limit $R(T)$ reaches minimum at $T^* \sim 0.7$ and then increases consistent with $R(T \rightarrow 0) \rightarrow \infty$ for a 2D system with $T = 0$ LRO. The same behavior appears for TL at $J_2 = 0$ with a shallow minimum shifted to $T^* \sim 0.3$. In contrast, results for KL as well as for TL with $J_2 = 0.1$ do not reveal such increase, at least not for $T > T_{fs}$, and they are more consistent with the interpretation that $R(T \rightarrow 0) \rightarrow 0$.

Finally, results for $R(T)$ within (S)EM are shown in

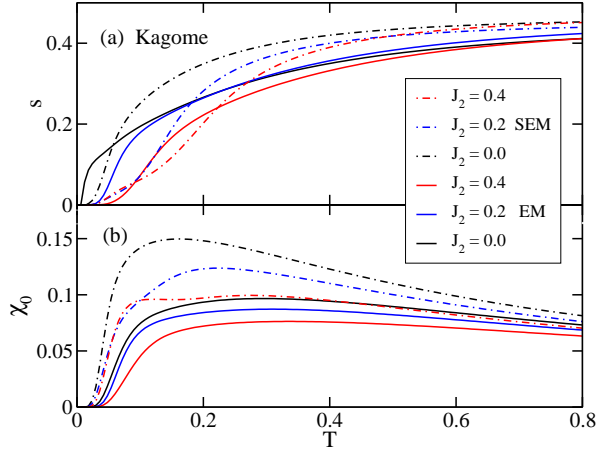


Figure 3. Results within EM and SEM on kagome lattice for different $J_2 = 0, 0.2, 0.4$; a) for $s(T)$, and b) $\chi_0(T)$.

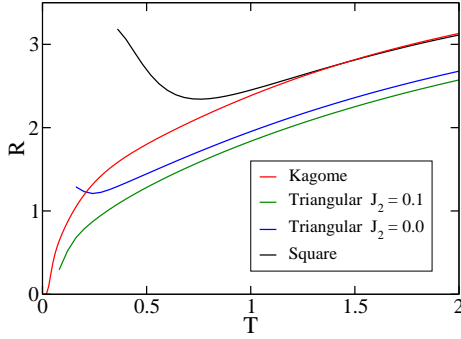


Figure 4. Wilson ratio $R(T)$, evaluated from $s(T)$ and $\chi_0(T)$ for full HM on square lattice, triangular lattice with $J_2 = 0, 0.1$ [54], and kagome lattice [48]. Results are presented for $T > T_{fs}$.

Fig. 5a,b as they follow from Fig. 2,3 for different $J_2 \geq 0$. We recognize that EM qualitatively reproduce numerical data within the full HM on Fig. 4. Although for $J_2 = 0$ TL results in Fig. 5a fail to reveal clearly the minimum down to $T_{fs} \sim 0.1$, there is still a marked difference to the SL regime $J_2 = 0.1, 0.15$ where EM confirms $R_0 \ll 1$. The SEM for TL apparently overestimates $R(T)$ at low T , due to too low $s(T)$. Results within (S)EM for KL, as shown in Fig. 5b, are even better demonstration. Here, for $J_2 = 0$ EM and SEM yield quite similar $R(T)$, decreasing and tending towards $R_0 \sim 0$. On the other hand, the effect of finite $J_2 > 0$ is well visible and leads towards LRO with $R_0 \rightarrow \infty$ for $J_2 = 0.4$, while again SEM presumably overestimates $R(T)$ for $J_2 = 0.2$.

Conclusions. Presented results for entropy $s(T)$, susceptibility $\chi_0(T)$ and in particular the Wilson ratio $R(T)$ reveal similarities between the HM in the SL regimes on TL and KL, apparently not stressed so far. The introduction of effective model delivers also a useful analytical insight. Apart from offering some numerical advan-

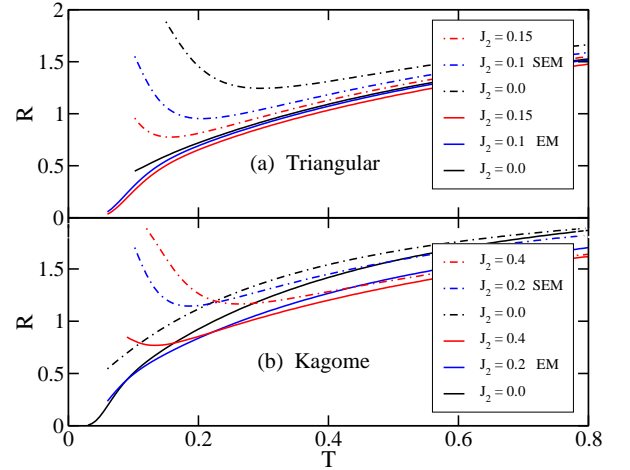


Figure 5. $R(T)$, evaluated within EM and SEM for: a) TL with $J_2 = 0, 0.1, 0.15$, and b) KL for $J_2 = 0, 0.2, 0.4$.

tages of reduced number of basis states, essential for ED methods, (S)EM clearly separate effective spin degrees s_i , determining $\chi_0(T)$, and chirality degrees τ_i which do not contribute to $\chi_0(T)$ but enter the entropy $s(T)$ and related specific heat. The essential common feature of SL regimes in HM on both lattices is a pronounced remanent $s(T) > 0$ at $T \ll J$, which within the (S)EM has the origin in dominant low-energy chiral fluctuations, well below the effective spin triplet gap Δ_t which is revealed by the drop of $\chi_0(T)$. As a consequence we observe the vanishing of the Wilson ratio $R_0 = R(T \rightarrow 0) \rightarrow 0$, which might be quite generic feature of 2D SL. Clearly, due to finite-size restrictions we could hardly distinguish a spin-gapped system from scenarios with more delicate gap structure which could also lead to renormalized $R_0 \ll 1$. Moreover, it is even harder to establish beyond finite-size the singlet gap $\Delta_s > 0$, which from $R(T)$ should nevertheless satisfy $\Delta_s < \Delta_t$.

Quantities discussed above are (in principle) measurable in real materials and have been indeed discussed for some of them. There are evident experimental difficulties, i.e., $\chi_0(T)$ can have significant impurity contributions while $s(T)$ may be masked by phonon contribution at $T > 0$. The essential hallmark for material candidates for the presented SL scenario should be a substantial entropy $s(T)$ persisting well below $T \ll J$. There are indeed several studies of $s(T)$ reported for different SL candidates (with some of them revealing transitions to LRO at very low T), e.g., for KL systems volborthite [10], $\text{YCu}_3(\text{OH})_6\text{Cl}_3$ [15], and recent TL systems 1T-TaS₂ [21] and Co-based SL materials [61]. Still, our model studies cannot exclude the relevant effect of additional terms, e.g., the Dzaloshinski-Moriya interaction [62, 63] and/or 3D coupling, which can reduce $s(T)$ or even induce LRO at $T \rightarrow 0$.

This work is supported by the program P1-0044 of the

Slovenian Research Agency. Authors thank J. Schnack for providing their data for kagome lattice and J. Schnack, F. Becca, A. Zorko, T. Morita and T. Tohyama for fruitful discussions.

-
- [1] P. W. Anderson, “Resonating valence bonds: a new kind of insulator?” *Mat. Res. Bull.* **8**, 153–160 (1973).
- [2] P. A. Lee, “An end to the drought of quantum spin liquids.” *Science (New York, N.Y.)* **321**, 1306–1307 (2008).
- [3] L. Balents, “Spin liquids in frustrated magnets,” *Nature* **464**, 199–208 (2010).
- [4] Lucile Savary and Leon Balents, “Quantum spin liquids: A review,” *Rep. Prog. Phys.* **80** (2017).
- [5] M. R. Norman, “Colloquium: Herbertsmithite and the search for the quantum spin liquid,” *Rev. Mod. Phys.* **88**, 041002 (2016).
- [6] P. Mendels, F. Bert, M. A. de Vries, A. Olariu, A. Harrison, F. Duc, J. C. Trombe, J. S. Lord, A. Amato, and C. Baines, “Quantum magnetism in the paratacamite family: Towards an ideal kagomé lattice,” *Phys. Rev. Lett.* **98**, 077204 (2007).
- [7] A. Olariu, P. Mendels, F. Bert, F. Duc, J. C. Trombe, M. A. de Vries, and A. Harrison, “ ^{17}O nmr study of the intrinsic magnetic susceptibility and spin dynamics of the quantum kagome antiferromagnet $\text{ZnCu}_3(\text{OH})_6\text{Cl}_2$,” *Phys. Rev. Lett.* **100**, 087202 (2008).
- [8] Tian Heng Han, Joel S. Helton, Shaoyan Chu, Daniel G. Nocera, Jose A. Rodriguez-Rivera, Collin Broholm, and Young S. Lee, “Fractionalized excitations in the spin-liquid state of a kagome-lattice antiferromagnet,” *Nature* **492**, 406–410 (2012).
- [9] M. Fu, T. Imai, T.-H. Han, and Y. S. Lee, “Evidence for a gapped spin-liquid ground state in a kagome heisenberg antiferromagnet,” *Science* **350**, 655–658 (2015).
- [10] Z. Hiroi, M. Hanawa, N. Kobayashi, M. Nohara, H. Takagi, Y. Kato, and M. Takigawa, “Spin-1/2 kagomé-like lattice in volborthite $\text{Cu}_3\text{V}_2\text{O}_7(\text{OH})_2 \cdot 2\text{H}_2\text{O}$,” *J. Phys. Soc. Jpn.* **70**, 3377–3384 (2001).
- [11] B. Fåk, E. Kermarrec, L. Messio, B. Bernu, C. Lhuillier, F. Bert, P. Mendels, B. Koteswararao, F. Bouquet, J. Ollivier, A. D. Hillier, A. Amato, R. H. Colman, and A. S. Wills, “Kapellasite: A kagome quantum spin liquid with competing interactions,” *Phys. Rev. Lett.* **109**, 037208 (2012).
- [12] Yuesheng Li, Bingying Pan, Shiyang Li, Wei Tong, Langsheng Ling, Zhaorong Yang, Junfeng Wang, Zhongjun Chen, Zhonghua Wu, and Qingming Zhang, “Gapless quantum spin liquid in the $s = 1/2$ anisotropic kagome antiferromagnet $\text{ZnCu}_3(\text{OH})_6\text{SO}_4$,” *New J. Phys.* **16**, 093011 (2014).
- [13] M. Gomilšek, M. Klanjšek, M. Pregelj, F. C. Coomer, H. Luetkens, O. Zaharko, T. Fennell, Y. Li, Q. M. Zhang, and A. Zorko, “Instabilities of spin-liquid states in a quantum kagome antiferromagnet,” *Phys. Rev. B* **93**, 060405(R) (2016).
- [14] Zili Feng, Zheng Li, Xin Meng, Wei Yi, Yuan Wei, Jun Zhang, Yan Cheng Wang, Wei Jiang, Zheng Liu, Shiyang Li, Feng Liu, Jianlin Luo, Shiliang Li, Guo Qing Zheng, Zi Yang Meng, Jia Wei Mei, and Youguo Shi, “Gapped Spin-1/2 Spinon Excitations in a New Kagome Quantum Spin Liquid Compound $\text{Cu}_3\text{Zn}(\text{OH})_6\text{FBr}$,” *Chin. Phys. Lett.* **34**, 077502 (2017).
- [15] A. Zorko, M. Pregelj, M. Klanjšek, M. Gomilšek, Z. Jagličić, J. S. Lord, J. A. T. Verezhak, T. Shang, W. Sun, and J. X. Mi, “Coexistence of magnetic order and persistent spin dynamics in a quantum kagome antiferromagnet with no intersite mixing,” (2019), arXiv:1904.02878.
- [16] Y. Shimizu, K. Miyagawa, K. Kanoda, M. Maesato, and G. Saito, “Spin liquid state in an organic Mott insulator with a triangular lattice,” *Phys. Rev. Lett.* **91**, 107001 (2003).
- [17] Y. Shimizu, K. Miyagawa, K. Kanoda, M. Maesato, and G. Saito, “Emergence of inhomogeneous moments from spin liquid in the triangular-lattice mott insulator $\kappa-(\text{ET})_2\text{Cu}_2(\text{CN})_3$,” *Phys. Rev. B* **73**, 140407(R) (2006).
- [18] T. Itou, A. Oyamada, S. Maegawa, and R. Kato, “Instability of a quantum spin liquid in an organic triangular-lattice antiferromagnet,” *Nat. Phys.* **6**, 673–676 (2010).
- [19] Y. Zhou, K. Kanoda, and T. K. Ng, “Quantum spin liquid states,” *Rev. Mod. Phys.* **89**, 025003 (2017).
- [20] M. Klanjšek, A. Zorko, R. Žitko, J. Mravlje, Z. Jagličić, P. K. Biswas, P. Prelovšek, D. Mihailovic, and D. Arčon, “A high-temperature quantum spin liquid with polaron spins,” *Nat. Phys.* **13**, 1130–1134 (2017).
- [21] M. Kratochvilova, A. D. Hillier, A. R. Wildes, L. Wang, S.-W. Cheong, and J.-G. Park, “The low-temperature highly correlated quantum phase in the charge-density-wave 1T-TaS₂ compound,” *Quantum Mat.* **2**, 42 (2017).
- [22] K. T. Law and P. A. Lee, “1T-TaS₂ as a quantum spin liquid,” *Proc. Nat. Ac. Sc.* **2017**, 201706769 (2017).
- [23] Wen-Yu He, Xiao Yan Xu, Gang Chen, K. T. Law, and Patrick A. Lee, “Spinon fermi surface in a cluster mott insulator model on a triangular lattice and possible application to 1t-tas₂,” *Phys. Rev. Lett.* **121**, 046401 (2018).
- [24] B. Bernu, P. Lecheminant, C. Lhuillier, and L. Pierre, “Exact spectra, spin susceptibilities, and order parameter of the quantum heisenberg antiferromagnet on the triangular lattice,” *Phys. Rev. B* **50**, 10048–10062 (1994).
- [25] L. Capriotti, A. E. Trumper, and S. Sorella, “Long-range néel order in the triangular heisenberg model,” *Phys. Rev. Lett.* **82**, 3899–3902 (1999).
- [26] Steven R. White and A. L. Chernyshev, “Neél order in square and triangular lattice heisenberg models,” *Phys. Rev. Lett.* **99**, 127004 (2007).
- [27] A. L. Chernyshev and M. E. Zhitomirsky, “Spin waves in a triangular lattice antiferromagnet: Decays, spectrum renormalization, and singularities,” *Phys. Rev. B* **79**, 144416 (2009).
- [28] R. Kaneko, S. Morita, and M. Imada, “Gapless spin-liquid phase in an extended spin 1/2 triangular Heisenberg model,” *J. Phys. Soc. Japan* **83**, 093707 (2014).
- [29] K. Watanabe, H. Kawamura, H. Nakano, and T. Sakai, “Quantum spin-liquid behavior in the spin-1/2 random heisenberg antiferromagnet on the triangular lattice,” *J. Phys. Soc. Japan* **83**, 034714 (2014).
- [30] Z. Zhu and White S. R., “Spin liquid phase of the $S=1/2$ J1-J2 Heisenberg model on the triangular lattice,” *Phys. Rev. B* **92**, 041105(R) (2015).
- [31] Wen-Jun Hu, Shou-Shu Gong, Wei Zhu, and D. N. Sheng, “Competing spin-liquid states in the spin- $\frac{1}{2}$ heisenberg model on the triangular lattice,” *Phys. Rev. B* **92**, 140403(R) (2015).
- [32] Y. Iqbal, W.-J. Hu, R. Thomale, D. Poilblanc, and

- F. Becca, “Spin liquid nature in the Heisenberg,” *Phys. Rev. B* **93**, 144411 (2016).
- [33] Shou-Shu Gong, W. Zhu, J.-X. Zhu, D. N. Sheng, and Kun Yang, “Global phase diagram and quantum spin liquids in a spin- $\frac{1}{2}$ triangular antiferromagnet,” *Phys. Rev. B* **96**, 075116 (2017).
- [34] F. Ferrari and F. Becca, “Dynamical structure factor of the J1-J2 Heisenberg model on the triangular lattice: magnons, spinons, and gauge fields,” (2019), arXiv:1903.05691.
- [35] F. Mila, “Low-energy sector of the kagome antiferromagnet,” *Phys. Rev. Lett.* **81**, 2356–2359 (1998).
- [36] R. Budnik and A. Auerbach, “Low-energy singlets in the heisenberg antiferromagnet on the kagome lattice,” *Phys. Rev. Lett.* **93**, 187205 (2004).
- [37] Y. Iqbal, F. Becca, and D. Poilblanc, “Valence-bond crystal in the extended kagome spin-1/2 quantum Heisenberg antiferromagnet: A variational Monte Carlo approach,” *Phys. Rev. B* **83**, 100404(R) (2011).
- [38] Yasir Iqbal, Federico Becca, Sandro Sorella, and Didier Poilblanc, “Gapless spin-liquid phase in the kagome spin- $\frac{1}{2}$ heisenberg antiferromagnet,” *Phys. Rev. B* **87**, 060405(R) (2013).
- [39] A. M. Läuchli, J. Sudan, and E. S. Sørensen, “Ground-state energy and spin gap of spin-1/2 kagomé-heisenberg antiferromagnetic clusters: Large-scale exact diagonalization results,” *Phys. Rev. B* **83**, 212401 (2011).
- [40] S. Yan, D. A. Huse, and S. R. White, “Spin-liquid ground state of the S=1/2 kagome Heisenberg antiferromagnet,” *Science* **322**, 1173 (2008).
- [41] S. Depenbrock, I. P. McCulloch, and U. Schollwöck, “Nature of the spin-liquid ground state of the $s = 1/2$ heisenberg model on the kagome lattice,” *Phys. Rev. Lett.* **109**, 067201 (2012).
- [42] A. M. Läuchli, J. Sudan, and R. Moessner, “The S=1/2 Kagome Heisenberg Antiferromagnet Revisited,” (2016), arXiv:1611.06990.
- [43] H. J. Liao, Z. Y. Xie, J. Chen, Z. Y. Liu, H. D. Xie, R. Z. Huang, B. Normand, and T. Xiang, “Gapless spin-liquid ground state in the $s = 1/2$ kagome antiferromagnet,” *Phys. Rev. Lett.* **118**, 137202 (2017).
- [44] N. Elstner and A. P. Young, “Spin-1/2 heisenberg antiferromagnet on the kagome lattice: High-temperature expansion and exact-diagonalization studies,” *Phys. Rev. B* **50**, 6871–6876 (1994).
- [45] P. Sindzingre, G. Misguich, C. Lhuillier, B. Bernu, L. Pierre, Ch. Waldtmann, and H.-U. Everts, “Magnetothermodynamics of the spin- $\frac{1}{2}$ kagomé antiferromagnet,” *Phys. Rev. Lett.* **84**, 2953–2956 (2000).
- [46] G. Misguich and P. Sindzingre, “Magnetic susceptibility and specific heat of the spin-1/2 Heisenberg model on the kagome lattice and experimental data on $\text{ZnCu}_3(\text{OH})_6\text{Cl}_2$,” *Eur. Phys. J. B* **59**, 305–309 (2007).
- [47] B. Bernu and C. Lhuillier, “Spin susceptibility of quantum magnets from high to low temperatures,” *Phys. Rev. Lett.* **114**, 057201 (2015).
- [48] J. Schnack, J. Schulenburg, and J. Richter, “Magnetism of the $n = 42$ kagome lattice antiferromagnet,” *Phys. Rev. B* **98**, 094423 (2018).
- [49] F. Kolley, S. Depenbrock, I. P. McCulloch, U. Schollwöck, and V. Alba, “Phase diagram of the J_1-J_2 heisenberg model on the kagome lattice,” *Phys. Rev. B* **91**, 104418 (2015).
- [50] S. Capponi, A. Läuchli, and M. Mambrini, “Numerical contractor renormalization method for quantum spin models,” *Phys. Rev. B* **70**, 104424 (2004).
- [51] N. Elstner, R. R. P. Singh, and A. P. Young, “Finite temperature properties of the spin-1/2 heisenberg antiferromagnet on the triangular lattice,” *Phys. Rev. Lett.* **71**, 1629–1632 (1993).
- [52] Marcos Rigol, Tyler Bryant, and Rajiv R. P. Singh, “Numerical linked-cluster algorithms. I. Spin systems on square, triangular, and kagome lattices,” *Phys. Rev. E* **75**, 061118 (2007).
- [53] Marcos Rigol and Rajiv R. P. Singh, “Magnetic susceptibility of the kagome antiferromagnet $\text{ZnCu}_3(\text{OH})_6\text{Cl}_2$,” *Phys. Rev. Lett.* **98**, 207204 (2007).
- [54] P. Prelovšek and J. Kokalj, “Finite-temperature properties of the extended heisenberg model on a triangular lattice,” *Phys. Rev. B* **98**, 035107 (2018).
- [55] Efstratios Manousakis, “The spin-1/2 heisenberg antiferromagnet on a square lattice and its application to the cuprous oxides,” *Rev. Mod. Phys.* **63**, 1–62 (1991).
- [56] See Supplemental Material for more details.
- [57] Cornelius Lanczos, “An iteration method for the solution of the eigenvalue problem of linear differential and integral operators,” *J. Res. Natl. Bur. Stand. B* **45**, 255–282 (1950).
- [58] J. Jaklič and P. Prelovšek, “Finite-Temperature conductivity,” *Phys. Rev. B* **50**, 7129 (1994).
- [59] J. Jaklič and P. Prelovšek, “Finite-temperature properties of doped antiferromagnets,” *Adv. Phys.* **49**, 1–92 (2000).
- [60] P. Prelovšek and J. Bonča, “Ground state and finite temperature lanczos methods,” in *Strongly Correlated Systems - Numerical Methods*, edited by A. Avella and F. Mancini (Springer, Berlin, 2013).
- [61] Ruidan Zhong, Shu Guo, Guangyong Xu, Zhijun Xu, and Robert J. Cava, “Strong quantum fluctuations in a quantum spin liquid candidate with a Co-based triangular lattice,” (2019), arXiv:1905.02115.
- [62] O. Cépas, C. M. Fong, P. W. Leung, and C. Lhuillier, “Quantum phase transition induced by dzyaloshinskii-moriya interactions in the kagome antiferromagnet,” *Phys. Rev. B* **78**, 140405(R) (2008).
- [63] Ioannis Rousochatzakis, Salvatore R. Manmana, Andreas M. Läuchli, Bruce Normand, and Frédéric Mila, “Dzyaloshinskii-moriya anisotropy and nonmagnetic impurities in the $s = \frac{1}{2}$ kagome system $\text{ZnCu}_3(\text{OH})_6\text{Cl}_2$,” *Phys. Rev. B* **79**, 214415 (2009).

Supplemental Material for: Similarity of thermodynamic properties of Heisenberg model on triangular and kagome lattices

P. Prelovšek^{1,2} and J. Kokalj^{3,1}

¹*Jožef Stefan Institute, SI-1000 Ljubljana, Slovenia*

²*Faculty of Mathematics and Physics, University of Ljubljana, SI-1000 Ljubljana, Slovenia*

³*Faculty of Civil and Geodetic Engineering, University of Ljubljana, SI-1000 Ljubljana, Slovenia*

In the Supplemental Material we provide the full description of the effective model as well as some more details concerning the numerical method.

I. THE EFFECTIVE MODEL

Starting with the extended $J_1 - J_2$ Heisenberg model, Eq. 2 in the main text, and using the restricted basis of $S = 1/2$ states on a single triangle, Eq. 3, we derive the effective model, Eq. 4, valid for both triangular lattice (TL) and the kagome lattice (KL),

$$H = \frac{1}{2} \sum_{i,d} \mathbf{s}_i \cdot \mathbf{s}_j (D + \mathcal{H}_{ij}^d), \quad (1)$$

$$\mathcal{H}_{ij}^d = F_d \tau_i^+ \tau_j^- + P_d \tau_i^+ + Q_d \tau_j^+ + T_d \tau_i^+ \tau_j^+ + \text{H.c.},$$

where i runs over all sites (triangles) in the new triangular lattice and $d = 1-6$ over all nn sites (triangles). It is significant that the (new) spin part is isotropic, i.e. $\mathbf{s}_i \cdot \mathbf{s}_j$ is SU(2) invariant, while the chirality operators are only of the XY type, i.e. only τ_i^+, τ_j^- enter. Note that taking into account only D, F_d terms Eq. (2) conserves both total $s_{tot}^z = \sum_i s_i^z$ but also $\tau_{tot}^z = \sum_i \tau_i^z$, while τ_{tot}^z is not conserved when also P_d, Q_d, T_d terms are taken into account.

Triangular lattice. As already given in Eq. 5 in the main text, the leading terms are given by

$$D = \frac{2}{9}J + \frac{1}{3}J_2, \quad F = -\frac{4}{9}J + \frac{4}{3}J_2 \quad (2)$$

Further terms directly depend on the direction d and are given by

$$\begin{aligned} P_1 &= -\frac{4}{9}J, & P_2 &= \frac{2}{9}\omega^*J, & P_3 &= -\frac{4}{9}\omega J, \\ P_4 &= \frac{2}{9}J, & P_5 &= -\frac{4}{9}\omega^*J, & P_6 &= \frac{2}{9}\omega J, \\ T_1 &= -\frac{4}{9}J, & T_2 &= -\frac{4}{9}\omega J, & T_3 &= -\frac{4}{9}\omega^*J \end{aligned} \quad (3)$$

with $T_{d+3} = T_d$ and $Q_d = P_{d+3}$, where we denote $\omega = \exp(i\phi)$ with $\phi = 2\pi/3$. It is worth noticing, that in P_d, Q_d, T_d terms J_2 does not enter. It can be also directly verified that such coupling averaged over all nn bonds vanish, i.e.,

$$\bar{P} = \frac{1}{6} \sum_d P_d = 0, \quad \bar{Q} = \bar{T} = 0, \quad (4)$$

which might indicate that these terms are less important. This is, however, only partially true since the latter terms

also play the role to distribute the increase of entropy $s(T)$ in a wider T interval.

Kagome lattice. In the KL one can introduce, without loosing the generality of the EM, also the third-neighbor exchange term (across the hexagons) with the coupling J_3 . Then D and F_d couplings are given by

$$D = \frac{1}{9}J + \frac{2}{9}J_2 + \frac{2}{9}J_3, \quad F_1 = \frac{4}{9}\omega J + \frac{8}{9}\omega^*J_2 + \frac{4}{9}J_3, \quad (5)$$

while $F_{d+1} = F_d^*$. We note that although F_d coupling is alternating, its average is nonzero, real and negative, i.e. $\bar{F} = (1/6) \sum_d F_d = \text{Re} F_d < 0$, at least for $J_2/J < 1/2$. Further terms are given by

$$\begin{aligned} P_1 &= -\frac{2}{9}J + \frac{2}{9}\omega^*J_2 - \frac{2}{9}\omega J_3, \\ P_2 &= -\frac{2}{9}\omega J + \frac{2}{9}\omega^*J_2 - \frac{2}{9}J_3, \\ P_3 &= -\frac{2}{9}\omega J + \frac{2}{9}J_2 - \frac{2}{9}\omega^*J_3, \\ P_4 &= -\frac{2}{9}\omega^*J + \frac{2}{9}J_2 - \frac{2}{9}\omega J_3, \\ P_5 &= -\frac{2}{9}\omega^*J + \frac{2}{9}\omega J_2 - \frac{2}{9}J_3, \\ P_6 &= -\frac{2}{9}J + \frac{2}{9}\omega J_2 - \frac{2}{9}\omega^*J_3, \end{aligned} \quad (6)$$

with $Q_d = P_{d+3}$ and

$$\begin{aligned} T_1 &= \frac{4}{9}\omega^*J - \frac{4}{9}\omega^*J_2 + \frac{4}{9}J_3, & T_2 &= \frac{4}{9}J - \frac{4}{9}J_2 + \frac{4}{9}J_3, \\ T_3 &= \frac{4}{9}\omega J - \frac{4}{9}\omega J_2 + \frac{4}{9}J_3, & T_{d+3} &= T_d. \end{aligned} \quad (7)$$

Again, terms which do not conserve τ_{tot}^z have the property $\bar{P} = \bar{Q} = \bar{T} = 0$.

II. NUMERICAL METHOD

In the evaluation of thermodynamical quantities we use the FTLM [1–3], which is based on the Lanczos exact-diagonalization (ED) method [4], whereby the Lanczos-basis states are used to evaluate the normalized thermodynamic sum

$$Z(T) = \text{Tr} \exp[-(H - E_0)/T], \quad (8)$$

(where E_0 is the ground state energy of a system). The FTLM is particularly convenient to apply for the calculation of the conserved quantities, i.e. operators A commuting with the Hamiltonian $[H, A] = 0$. In this way we evaluate Z , the thermal average energy $\Delta E = \langle H - E_0 \rangle$, magnetization $\bar{M} = \langle s_{tot}^z \rangle$ (nontrivial, e.g., in the presence of additional external field $h > 0$ and square of magnetization $M^2 = \langle [s_{tot}^z]^2 \rangle$). From these quantities we evaluate the thermodynamic observables of interest, i.e. uniform susceptibility $\chi^0(T)$ and entropy density $s(T)$,

$$\chi^0 = \frac{M^2}{NT}, \quad s = \frac{T \ln Z + \Delta E}{NT}, \quad (9)$$

where N is the number of sites in the original lattice.

We note that for above conserved operators A , commuting with the Hamiltonian $[H, A] = 0$, there is no need to store Lanczos wavefunctions, so the requirements

are essentially that of the g.s. Lanczos ED method, except that the summation over all symmetry sectors and a modest sampling $N_s < 10$ over initial wavefunctions is helpful. As symmetries we take into account explicitly the translation symmetry (for given q), s_{tot}^z , and for SEM also τ_{tot}^z . In such framework we can reach system sizes with $N_{st} < 10^8$ basis states, which means EM with up to $N = 42$ sites and SEM with up to $N = 48$ sites.

The main criterion for the macroscopic relevance of FTLM results is $Z(T) \gg 1$ (at least for system where gapless excitation are expected), which in practice leads to a criterion $Z > Z^* = Z(T_{fs}) \gg 1$. Taking $Z^* \sim 20$ implies (for $N = 42$) also roughly the threshold entropy density $s(T_{fs}) \sim 0.07$, independent of the model. It is then evident that the actual T_{fs} depends crucially on the model, so that large $s(T)$ works in favor of using FTLM for frustrated and SL systems. Moreover, in the case of models with a sizeable gap, e.g. $\Delta > T_{fs}$ the results of FTLM can be reliable even down to $T \rightarrow 0$ [2].

-
- [1] J. Jaklič and P. Prelovšek, *Phys. Rev. B* **50**, 7129 (1994).
 - [2] J. Jaklič and P. Prelovšek, *Adv. Phys.* **49**, 1 (2000).
 - [3] P. Prelovšek and J. Bonča, in *Strongly Correlated Systems - Numerical Methods*, edited by A. Avella and F. Mancini

- (Springer, Berlin, 2013).
- [4] C. Lanczos, *J. Res. Natl. Bur. Stand. B* **45**, 255 (1950).